

**INVITED TALK**

Presented at  
*The International Conference on Metallurgical Coatings and Thin Films*  
(ICMCTF 2003)  
San Diego, April 28 - May 2, 2003

A reviewed version may be accepted at  
*Surface and Coatings Technology*

**Fundamentals of Pulsed Plasmas for Materials Processing**

**André Anders**

Lawrence Berkeley National Laboratory, University of California,  
1 Cyclotron Road, Berkeley, California 94720-8223

Abstract: October 23, 2002  
April 27, 2003

Corresponding Author:

André Anders  
Lawrence Berkeley National Laboratory  
1 Cyclotron Road, MS 53  
Berkeley, CA 94720-8223  
Tel. (510) 486-6745  
Fax (510) 486-4374  
e-mail [aanders@lbl.gov](mailto:aanders@lbl.gov)

This work was supported by the Assistant Secretary for Energy Efficiency and Renewable Energy, Office of Building Technology, of the U.S. Department of Energy under Contract No. DE-AC03-76SF00098.

# **Fundamentals of Pulsed Plasmas for Materials Processing**

**André Anders**

Lawrence Berkeley National Laboratory, University of California,

1 Cyclotron Road, Berkeley, California 94720-8223

## **Abstract**

Pulsed plasmas offer the use of much higher power (during each pulse) compared to continuously operated plasmas, and additional new parameters appear such as pulse duty cycle. Pulsed processing may help meeting the demands of increasingly sophisticated materials processes, including thin film deposition, plasma etching, plasma cleaning of surfaces, and plasma immersion ion implantation. The high kinetic energy of ions allows processes to occur far from thermodynamic equilibrium. Pulsed plasmas are driven by external pulsed power sources, and one has to consider the power source and the plasma as a coupled system. The dynamic plasma impedance is a key quantity from an electrical engineering point of view. From a plasma physics point of view, one needs to consider the dynamics of plasma species, their density and energy distribution, ionization and recombination reactions, and, most importantly, the development of transient sheaths. Dimensionless scaling parameters are a useful tool putting the variety of plasma parameters in relation to characteristic quantities. This is illustrated by several examples of pulsed processes relevant to thin film deposition. The emerging technology of pulsed sputtering is discussed in detail including the possibility to achieve the mode of self-sustained self-sputtering during each pulse.

## 1. Introduction

Coating processes that involve plasma have been used for over a century but their full potential has yet to be exploited. Over the last decades, tremendous progress has been made in understanding and utilization of plasma to obtain coatings and surfaces with desired properties. For example, plasmas have been introduced in plasma-assisted CVD and PVD (chemical and physical vapor deposition, respectively), leading to coatings of much improved quality [1, 2]. Improvements are generally attributed to “activation” of condensing particles and enhancement of surface mobility, which usually leads to denser films, affecting a wide range of mechanical, optical, electrical and other properties. To further optimize properties of coatings and surface structures, plasma can be “engineered,” and this is the topic of following overview, with emphasis on *pulsed* plasmas. In the following sections, a summary of important plasma laws and parameters is provided. Readers well familiar with plasmas may skip this section and go the main part devoted to deriving conclusions from basic considerations for pulsed operation of processing plasmas.

## 2. Basic laws and characteristic parameters of plasmas

Before the effects on plasmas on surfaces and growing films are discussed, it is useful to very briefly recall some basic laws and parameters of plasmas (for exact derivations see textbooks on plasmas, e.g. [3-5]). A plasma can be roughly defined as an ensemble of particles with long range interaction, such as Coulomb interaction between charged particles. Many macroscopic properties are determined by collective interaction of particles. The ensemble is quasi-neutral,

$$\sum_{\alpha} Q_{\alpha} n_{\alpha} - n_e - \sum_{\beta} Q_{\beta} n_{\beta} = 0, \quad (1)$$

where the indices  $\alpha$  and  $\beta$  refer to the kinds of positive and negative ions present, whose charge state number and density are denoted by  $Q$  and  $n$ , respectively. In many cases, only singly charged, positive ions are present, and one can simplify (1) to

$$n_e = n_i. \quad (2)$$

The long-range Coulomb potential of a charged particle in a plasma is shielded by the presence of neighboring charged particles. The characteristic shielding length is the electron Debye length

$$\lambda_{De} = \left( \frac{\epsilon_0 k T_e}{n_e e^2} \right)^{1/2}. \quad (3)$$

The symbols in Eq. (3) have their usual meaning, namely  $\epsilon_0 \approx 8.854 \times 10^{-12}$  F/m is the permittivity of free space,  $k \approx 1.38 \times 10^{-23}$  J/K is Boltzmann's constant, and  $e \approx 1.60 \times 10^{-19}$  C is the elementary charge. Assuming typical values of processing plasmas, for example argon plasma with  $kT_e \approx 2-3$  eV and  $n_e \sim 10^{15} - 10^{17}$  m<sup>-3</sup>, one finds that the Debye length is relatively short, in the range 33-410  $\mu$ m in the example. To qualify as plasma, the size of the ensemble of charged particles has to be much larger than its Debye length. The condition of quasi-neutrality, Eqs. (1) or (2), is not valid on a length scale of order  $\lambda_{De}$  and smaller, and therefore large electric fields can exist and lead to changes of the trajectories of charged particles (Coulomb collisions).

A momentary local imbalance of positive and negative charge will cause a large electric field. The field can be calculated by the Poisson equation, which is the third in the set of Maxwell equations, written in macroscopic form as:

$$\nabla \times \mathbf{E} = -\mu_0 \frac{\partial \mathbf{H}}{\partial t} \quad (4)$$

$$\nabla \times \mathbf{H} = \epsilon_0 \frac{\partial \mathbf{E}}{\partial t} + \mathbf{J} \quad (5)$$

$$\epsilon_0 \nabla \cdot \mathbf{E} = \rho \quad (6)$$

$$\mu_0 \nabla \cdot \mathbf{H} = 0 \quad (7)$$

where  $\mathbf{E}(\mathbf{r}, t)$  and  $\mathbf{H}(\mathbf{r}, t)$  are the space and time dependent electric and magnetic field vectors, and  $\mu_0 = 4\pi \times 10^{-7}$  H/m is the permeability of free space. The net charge density  $\rho = n_i - n_e$  and the current density  $\mathbf{J}(\mathbf{r}, t)$  are the sources of electric and magnetic field, respectively. Charge density and current are not independent but related by the continuity equation

$$\frac{\partial \rho}{\partial t} + \nabla \cdot \mathbf{J} = G - L \quad (8)$$

where  $G$  and  $L$  are the gain and loss terms describing ionization and recombination.

Because electrons are much lighter than ions, they respond to a change in the electric field much

faster, and they will quickly move in such a way as to minimize the local net charge  $\rho$ . They will overshoot the equilibrium position and create now local charge, thus leading to oscillatory motion characterized by the electron plasma frequency

$$\omega_{pl,e} = \left( \frac{n_e e^2}{\epsilon_0 m_e} \right)^{1/2}. \quad (9)$$

Using again the example of  $n_e \sim 10^{15} - 10^{17} \text{ m}^{-3}$  one obtains about  $\omega_{pl,e} = 1.8 - 18 \times 10^9 \text{ s}^{-1}$ . The inverse is 56-560 ps, a very short time, and one can immediately see that electrons will do many oscillations on timescales of macroscopic changes.

While oscillating, the electron may encounter a collision with another electron, ion, or neutral atom or molecule. In general, the probability of a collision depends on the relative velocity of the colliding particles,  $u$ , the density of target particles (i.e. particles to be hit),  $n_\beta$ , and the cross section of interaction  $\sigma_{\alpha\beta}(u)$ . Collision theory [4, 6, 7] uses the concept of mean-free-path,  $\lambda_\alpha$ , the mean distance between collisions of particle of type  $\alpha$  with other particles

$$\lambda_\alpha = \left( \sum_\beta n_\beta \sigma_{\alpha\beta} \right)^{-1}. \quad (10)$$

The mean time between collisions is

$$\tau_\alpha = \frac{\lambda_\alpha}{u}. \quad (11)$$

The mean frequency of collisions is the inverse, i.e.,

$$\tau_\alpha^{-1} = \frac{u}{\lambda_\alpha} = \sum_\beta n_\beta \sigma_{\alpha\beta} u. \quad (12)$$

When averaged over all velocities of the (usual Maxwell) distribution one obtains the collision frequency

$$\nu_\alpha = \sum_\beta n_\beta \langle \sigma_{\alpha\beta} u \rangle. \quad (13)$$

where the averaging is performed as

$$\langle \sigma_{\alpha\beta} u \rangle = \frac{1}{n_\alpha} \int_{-\infty}^{\infty} \sigma_{\alpha\beta}(u) u f_\alpha(u) du. \quad (14)$$

Using the cross section of Debye-shielded Coulomb interaction between charged particles, Spitzer [8] calculated the momentum transfer collision frequencies for electrons and ions as:

$$\nu_{ab} \approx C \frac{Q_a^2 Q_b^2}{m_a^{1/2} (kT_a)^{3/2}} n_b \quad (15)$$

where the indices  $a$  and  $b$  stand for any combination of electrons and ions,  $Q$  is the charge state number (for electrons  $Q_e^2 = 1$ ); the constant  $C = \frac{e^4 \ln \Lambda}{12\pi^{3/2} \epsilon_0^2} \approx 1.3 \times 10^{-54} (\text{AsVm})^2$  contains the Coulomb logarithm  $\ln \Lambda \approx 10$ , a quantity related to shielding of the interaction potential. Our example argon plasma would give the following ranges for momentum transfer collision frequencies:  $\nu_{ee} \approx \nu_{ei} \approx 10^3 - 10^5 \text{ s}^{-1}$ , and  $\nu_{ii} \approx 10^4 - 10^6 \text{ s}^{-1}$ .

Collisions can be elastic or inelastic. Elastic collisions are those where the total kinetic energy of colliding particles is conserved, while inelastic collisions are associated with energy transfer to “inner” degrees of freedom, e.g. ionization and excitation. The cross section for these collisions can be vastly different, and therefore one has to distinguish between mean free paths and collision frequencies specific to types of collision processes.

Additional effects occur in the presence of a magnetic field. Electrons execute gyration motion with the gyration frequency

$$\omega_e = eB/m_e \quad (16)$$

where  $B$  is the magnetic inductance. An electron having a velocity component  $u_{e\perp}$  perpendicular to  $\mathbf{B}$  will have a gyration radius

$$r_{g,e} = \frac{u_{e\perp}}{\omega_e} = \frac{m_e u_{e\perp}}{eB} \quad (17)$$

Ion motion in magnetic fields follows the same laws but the ion mass and velocity has to be used. In most processing plasmas with external magnetic fields, the field is not strong enough to make the ion gyration radius small compared to the system dimension. In these cases, one speaks of plasmas with magnetized electrons but non-magnetized ions.

### 3. Sheaths

While the bulk of plasma is quasi-neutral, its boundary layer is not. Boundary layers (sheaths) appear where a plasma meets a solid such as a chamber wall, substrate, or probe. The structure of a sheath depends on the potential difference between the solid surface and the plasma potential. Unless this difference is externally driven, a space charge will quickly establish itself in such a way as to balance particle fluxes through the sheath. The case of a floating object is particularly easy to comprehend: the net current must be zero, thus the space charge must balance the flow of positive and negative charges. The electron current from the plasma is determined by thermal random motion

$$j_e = \frac{1}{4} e n_{es} \bar{u}_e \exp\left(\frac{eV_0}{kT_e}\right) \quad (18)$$

where  $V_0 < 0$  is the potential of the surface with respect to the plasma potential,  $n_{es}$  is the electron density at the sheath edge, and

$$\bar{u}_e = \left(\frac{8kT_e}{\pi m_e}\right)^{1/2} \quad (19)$$

is the electron velocity averaged over a Maxwell distribution. The ion current is

$$j_i = \bar{Q} e n_{is} u_{is}, \quad (20)$$

where  $\bar{Q}$  is the average ion charge state. The velocity of ions at the sheath edge,  $u_{is}$ , is known as the Bohm velocity [9]

$$u_{is} = u_{Bohm} = \left(\frac{kT_e}{m_i}\right)^{1/2}, \quad (21)$$

which is greater than the random velocity due to acceleration in the presheath, i.e. the zone between undisturbed plasma and the sheath [10]. From the condition  $j_e = j_i$  one obtains the potential of the wall with respect to the plasma potential

$$V_{float} = -\frac{kT_e}{2e} \ln\left(\frac{m_i}{2\pi m_e}\right). \quad (22)$$

To illustrate the above equations, we consider again our argon model plasma. The resulting quantities are:

$$\bar{u}_e \approx 0.9 - 1.2 \times 10^6 \text{ m/s}, \quad u_{is} = u_{Bohm} \approx 2200 - 2700 \text{ m/s}, \quad V_{float} = -(9 - 14) \text{ V}, \quad j_i \approx j_e \approx 1 \text{ A/cm}^2.$$

Now we consider a situation when a wall is biased and a net current of charged particles flows to the wall. Assuming that the particle energy outside the sheath is much smaller than the potential drop in the sheath, Child [11] and later Langmuir [12] solved Poisson's equation and the continuity equation finding that space charge limits the current. Considering a negative wall potential, the Child law for space-charge limited ion current can be written as [13]

$$j_i = \frac{4}{9} \epsilon_0 \left( \frac{2e}{m_i} \right)^{1/2} \frac{V_0^{3/2}}{s^2}, \quad (23)$$

where  $V_0$  is the absolute value of the sheath potential (voltage drop across the sheath). A common interpretation (and application) of Child's law is for vacuum diodes and ion extraction systems where  $s$  is the fixed distance between positive and negative electrode, and  $j_i$  represents the maximum ion current possible. More relevant for surface engineering is the situation when a substrate is biased negatively with respect to the plasma potential and the ion current is determined by the supply from the plasma, Eq. (20). Given enough time (to be discussed later), the sheath becomes a *Child law sheath* with the thickness

$$s_{Child} = \frac{\sqrt{2}}{3} \lambda_{De} \left( \frac{2eV_0}{kT_e} \right)^{3/4}. \quad (24)$$

Considering again the argon model plasma mentioned before, one obtains  $s_{Child} = 1.7 - 27 \text{ mm}$ .

#### 4. Dimensionless parameters

The use of dimensionless parameters is a powerful technique to evaluate and understand plasma parameters, scaling, and dynamic behavior. The idea is not new but well developed, for example, in fluid and gas dynamics. Essentially, one selects the most important characteristic physical quantity and normalizes other quantities of the same dimension. Dimensionless parameters relevant for pulsed plasma processing are compiled in Table 1. In a *dynamic* plasma situation, usually both the normalized and the normalizing quantities change. The elegance and power of dimensionless parameters is to be able to immediately evaluate a physical situation. For example, in assessing the collisionality in the sheath region, one could chose the sheath thickness as the normalizing quantity and investigate the mean free path in



relation to the sheath thickness when the pulse voltage is changed.

For dynamic situations, the pulse duration, or fall and rise times, are often compared with, for example, the characteristic response time of an equilibrium value  $q_{equ}$ , the latter can generally be expressed as

$$\tau = \left| \frac{1}{q_{equ}} \frac{dq_{equ}}{dt} \right|^{-1}. \quad (25)$$

If  $\tau$  is small compared to the pulse times, the plasma system goes in a new equilibrium state as dictated by the pulse parameters, the opposite case the plasma system is in non-equilibrium. This concept will be illustrated below.

## 5. Pulsed plasmas and pulsed sheaths

### 5.1. General considerations for pulsed systems

When considering pulsed systems, new parameters appear, specifically pulse duration and duty cycle. Other parameters will be changed significantly compared to non-pulsed operation, for example the amplitude of current can be orders of magnitude higher, leading to higher power and particle energies, higher degree of ionization of the plasma, and other effects. One needs to distinguish between values during a pulse and during pulse-off time, or peak versus average values.

The duty cycle of a pulse train is defined by the relative duration of the pulse-on time,

$$\delta = \frac{t_{on}}{t_{on} + t_{off}}. \quad (26)$$

For pulses with almost rectangular shape one would use the FWHM (full width at half maximum) as the relevant on-time. For irregularly shaped pulses, or more sine-like shapes, the term duty cycle is not well suited.

If the duty cycle concept is applicable, average values can be easily determined from peak values using

$$\bar{A} = A \delta \quad (27)$$

where  $A$  stands for any physical quantity, such as power. If the pulse rise and fall times are not much shorter than the constant portion of the pulse, or no constant portion exists, the general averaging method

needs to be applied:

$$\bar{A} = \int_{t_1}^{t_2} A(t) dt / (t_2 - t_1) \quad (28)$$

where averaging occurs over the time interval  $(t_1, t_2)$ .

An advantage of pulsed system is that additional “knobs” exist for process optimization, and since plasma parameters are shifted, qualitatively different (hopefully better or superior) coatings and surfaces can be achieved.

Disadvantages of pulsed systems are higher cost, e.g. for the pulse modulator, and the need for higher voltage insulation, greater current capabilities of cables, better shielding against electromagnetic interference, pulsed magnetic fields, eddy currents, induced voltage spikes, and better cooling of components and electrodes.

With the above background knowledge in mind, various situations in pulsed plasma processing will be considered.

## 5.2. DC and pulsed substrate bias

Substrate bias has been used for many decades. Bias is usually of negative polarity to attract positive ions from the processing plasma. The goals are either preparation the substrate for the coating by sputtering, or improvement of the coating by ion bombardment. An example of the preparation goal can be found in the first phase of the ABS (arc bond sputtering) technology [14]. Ion plating [15] is an example for ion bombardment by biasing during film growth. Over the last decade, pulsed bias has become popular for several reasons. One is that the likelihood of unwanted substrate arcing is greatly reduced when using bias with short pulses, which is due to the time an emission site takes to become overheated and thus unstable. Other reasons are associated with the nature of pulsing, giving the option for higher voltage and high peak power while keeping the average power in the usual range.

Historically, the application of pulsed substrate bias has originated from several ideas and approaches. One is the technique of plasma immersion ion implantation (PIII), developed in the 1980s by Adler [16], Conrad [17], Mizuno [18], and others. By lowering pulsed bias from 10’s of kV to much smaller values, and using condensable metal plasmas, plasma immersion technology was expanded into the

field of interface engineering and film formation by energetic condensation [19]. A similar result was obtained by Olbrich et al. [20, 21] who started from ion plating with negative DC bias and superimposed pulsed bias. These techniques have been reviewed recently [22-25].

### 5.3. Transient sheaths

When a high negative potential is applied to a substrate, the electrons near the substrate are repelled on the timescale of the inverse electron plasma frequency, Eq.(9). The much more massive ions respond slower, namely on the timescale of the inverse ion plasma frequency:

$$\omega_{pl,i}^{-1} = \left( \frac{n_i \overline{Q^2} e^2}{\epsilon_0 m_i} \right)^{-1/2}. \quad (29)$$

The electron response time is in the nanosecond or even subnanosecond range, and it is save to say that all practical pulse rise times are longer. The situation for ions is more complicated. Here it is useful to consider the dimensionless parameter

$$\tau_{rise} = t_{rise} \omega_{pl,i}. \quad (30)$$

When  $\tau_{rise} \ll 1$ , electrons are repelled into the plasma, leaving a matrix of “exposed” ions behind. This is the famous *ion matrix sheath* that exists only for times shorter than  $\omega_{pl,i}^{-1}$ . Conrad and coworkers [17, 26] and Lieberman [27] derived formula for the ion matrix sheath, the simplest reads for plane geometry [28]

$$s_{IM} \approx \left( \frac{2\epsilon_0 V_0}{en_i} \right)^{1/2}. \quad (31)$$

For  $t > \omega_{pl,i}^{-1}$  ions move towards the substrate and electrons at the sheath edge continue to be repelled into the bulk plasma, thereby “uncovering” new ions and shifting the sheath edge further away from the substrate surface. If we neglect, for the time being, the velocity component of plasma ions arriving at the sheath edge, one can write the sheath position as [28]

$$s = s_{IM} \left( 1 + \frac{2}{3} \omega_{pl,i} t \right)^{1/3}. \quad (32)$$

According to this expression, sheath expansion slows down with time but appears to continue expansion forever, which of course is not true. The velocity of the sheath edge,  $ds/dt$ , also known as *sheath velocity*,

can be highly supersonic initially. As soon as it slows down and become comparable to the ion velocity in the plasma, Eq.(32) cannot be used. Assuming that the current to the substrate is composed of ions “uncovered” by the expanding sheath *and* by the ion flux from the plasma, Eq.(20), the sheath velocity can be written as [27]

$$\frac{ds}{dt} = \frac{2}{9} \frac{s_{IM}^2}{s^2} u_0 - u_{Bohm} \quad (33)$$

where  $u_0 = (2QeV_0/m_i)^{1/2}$  is the velocity ions have gained in the sheath. From (33) we can see that with increasing sheath thickness,  $s(t)$ , the first term of the rhs will become smaller in time until the sheath becomes stationary,  $ds/dt = 0$ . The stationary sheath is known as the already introduced Child law sheath, whose thickness can also be written as [28]

$$s_{Child} = s_{IM} \left( \frac{2}{9} \frac{u_0}{u_{Bohm}} \right)^{1/2}. \quad (34)$$

One could plug the Child thickness (34) in the simplified equation (32) to obtain an approximate expression for the time it takes to form a Child law sheath [28]:

$$t_{Child} \approx \frac{\sqrt{2}}{9} \omega_{pl,i}^{-1} \left( \frac{2eV_0}{kT_e} \right)^{3/4}. \quad (35)$$

So far, after Eq.(30), we have considered fast rising pulses with  $\tau_{rise} \ll 1$ . In the opposite case, when  $\tau_{rise} \gg 1$ , inertia of ions is not really important: Ions are able to respond to the slow rise in voltage and will establish the equilibrium Child law sheath at any time for the voltage at that time. For our argon model plasma we obtain  $\omega_{pl,i}^{-1} = 15-150$  ns. We see that the discussion of ion matrix sheaths, prevalent in many texts on plasma immersion processing, is only of limited relevance because rise times of most pulse systems are much longer than 1  $\mu$ s. If a fast bias pulser is available and  $\tau_{rise} \sim 1$ , the sheath thickness will be smaller than the equilibrium Child law thickness corresponding to the momentary voltage  $V_0(t)$ , but it will be close to it for  $t > t_{Child}$ . For the model argon plasma and a bias of  $-500$  V,  $t_{Child} \approx 200-750$  ns. This time is very short and the case  $\tau_{rise} \gg 1$  appears indeed to be common, and discussions of the ion matrix sheath an educational exercise rather than reality.

After the sheath has been established and reached equilibrium, one needs to discuss the collapse of

the sheath when the bias voltage is turned off with a characteristic fall time  $t_{fall}$ . Since  $t_{fall} \gg \omega_{pl,e}^{-1}$  for all practical situations, electrons from the plasma will fill the ion space charge in the sheath in an equilibrium manner, i.e. a Child law sheath with thickness (24) exists at any time corresponding to the momentary, now falling voltage  $V_0(t)$ . In analogy to  $\tau_{rise}$  one can introduce the dimensionless parameter

$$\tau_{fall} = t_{fall} \omega_{pl,i} \quad (36)$$

If  $\tau_{fall} \gg 1$ , ions from the plasma will move towards the substrate and “refill” the region that used to be the sheath. For  $\tau_{fall} \sim 1$  or even  $\tau_{fall} < 1$ , a quasi-neutral plasma is reestablished through electron motion as mentioned above, however, the initial local plasma density profile corresponds to the ion density profile of the sheath, with a density much lower than the plasma bulk density. Ambipolar diffusion of ions and electron will set in, eventually restoring the density profile as it existed before the pulse. The characteristic time of restoration is

$$t_{restore} \approx \frac{s_{Child}^2}{D_{ambi}} \quad (37)$$

where  $s_{Child}$  is the maximum sheath thickness (34) that was reached before the pulse was switched off;

$$D_{ambi} \approx kT_e \mu_i / e \quad (38)$$

is the ambipolar diffusion coefficient which is determined by the ion mobility [3]

$$\mu_i = \frac{e}{m_i \nu_i} \quad (39)$$

which in turn is determined by the momentum transfer collision frequency  $\nu_i$ , see Eq.(13).

The bias fall time is usually many microseconds or longer, and  $\tau_{fall} \gg 1$  applies in most case, hence possible positive charge accumulation on the surface can be compensated by the electrons supplied by the plasma. However, ambipolar diffusion to restore the original plasma density is slower, and so it is important to consider the duration of the pulse-off time. If  $t_{off} < t_{restore}$  the plasma density near the pulsed biased object is not fully restored. It is indeed possible that the duty cycle is sufficiently high, hence, the sheath of successive pulses propagate in increasingly thinner plasma, and thus the sheath edge extends further from the surface with each pulse until equilibrium is reached between “pumping” of ions by the bias pulse and supply by the plasma. Such multiple-pulse effects have been modeled for plasma immersion ion implantation using a particle-cell-code [29] but the principle also applies to other pulsed systems like pulsed sputtering.

The discussion above assumed negative bias. In the case of positive bias, electrons of plasma are attracted, which may be desirable e.g. to compensate for local charging of semi-conducting or insulating layers or to achieve surface heating. Similar to the collapsing sheath situation above, electrons will respond on the timescale  $\omega_{pl,e}^{-1}$ , which is much faster than any changes in bias, and therefore the corresponding current and sheaths changes can be described by equilibrium conditions. Prior to application of positive bias, the sheath between substrate and plasma is of order a few Debye lengths, Eq. (3). Due to the high mobility of electrons, positive bias will not increase sheath thickness considerably unless the bias generator can handle the very large electron current that can be drawn from the plasma, Eq.(18). In this case, a new situation may arise, namely that the bias generator becomes part of the plasma-generating system, rather than the plasma-utilizing system.

## 6. Selected examples of pulsed plasma processing

### 6.1. Plasma Immersion Ion Processing (PIIP)

Any electrode or substrate biased with  $V_0$  respect to the plasma will dissipate energy into the discharge system. The power is of order  $V_0 I_{bias}$ , where  $I_{bias}$  is the current caused by the bias. Part of this power will dissipate as heat in the biased electrode or substrate, and another part can contribute to plasma generation. One direct plasma generation mechanism is that electrons emitted from the surface are accelerated in the sheath, penetrate the plasma and make an ionizing collision, thereby increasing the plasma density and electron temperature. Changes in density and temperature affect the particle flux to the biased substrate and the sheath thickness. In conventional DC operation, substrates biased negatively draw an ion current that is small compared to the discharge current, and no dramatic changes occur. In contrast, pulsed operation can be used to determine plasma parameters. Plasma Immersion Ion Processing (PIIP) is one example where this concept is realized [30]. Here, the high negative pulsed bias applied to the substrate is to not only accelerating ions to the substrate surface but also assisting ion generation by accelerating secondary electrons in the sheath. The working gas density (i.e. pressure) must be sufficiently high, making the electron mean-free-path (10) sufficiently short, and the process gas must contain or decompose into condensable species. Typical gases are carbon-containing such as acetylene [31], leading

a-C:H films, or gas mixtures leading to doped films [32], or metallo-organic precursor gases e.g. for TiCN [33] and ZrCN coatings [34]. PIIP can be viewed as pulsed-plasma assisted CVD.

## 6.2. Pulsed magnetron sputtering

The possibility to obtain plasma containing ionized sputtered material for optimized film growth was the main driving force for the recent development of pulsed magnetron sputtering. Kouznetsov and coworkers [35] showed that by increasing the power density to a magnetron by orders of magnitude, from typically  $< 50 \text{ W/cm}^2$  to more than  $2 \text{ kW/cm}^2$ , significant ionization of the sputtered metal can be obtained, which is important when substrate biasing is used to control the energy of film-forming species, which, for example, is crucial for via and trench filling of semiconductors [36]. To avoid overheating of the magnetron, the average power density should be comparable to normal DC or RF operation. The degree of metal ionization is subject to research and will depend, apart from the power density, on the specifics of the system such as target material, gas pressure, pulse rise time, duration, frequency, etc. Measurements have significant uncertainty but indicate  $\alpha = 10\% - 70\%$  for power densities of order  $1\text{-}3 \text{ kW/cm}^2$  [35, 37, 38]. For comparison, less than 1% of titanium atoms were found to be ionized when Ti was DC-sputtered with Ar/N<sub>2</sub> at typical target power densities of about  $10 \text{ W/cm}^2$  [39].

It is insightful to study the current-voltage characteristic of the pulsed high-current, high-voltage discharge because it shows that it is necessary to consider the power supply and discharge plasma as a coupled system. Although voltage is driving electric current, it is customary for a good reason that the discharge characteristic is plotted as current-voltage and not voltage-current. The current in a plasma is typically determined by the current capability of the power supply, and not limited by the conductivity (better impedance, i.e. complex resistance) of the plasma. The voltage of the discharge (plasma plus sheaths) will establish itself only as high as needed to transport the current that is mainly determined by the rest of the circuit. In this sense, the current is the independent and the discharge voltage the dependent variable. Understanding this is important because discharge current and voltage will determine the power input, plasma parameters, and therefore ultimately the process parameters for film growth.

It is known (e.g. [5] p.343) that a typical sputtering system of relatively low current and power density shows a discharge characteristic

$$I_d = cV_d^q \quad (40)$$

where typically  $q = 2-12$ ,  $c$  is a constant, and  $V_d$  is the voltage between anode and cathode. A high index  $q$  means that the discharge can easily accommodate a higher current with very little change in voltage. It can do that because the plasma is only partially ionized and generates more charge carriers as needed. In fact, glow discharge characteristics can be flat and may become negative, meaning that higher currents create plasma and sheath of lower impedance, with the possibility to transition into an arc, the latter being accompanied by a completely new mechanism of plasma generation at cathode spots [40].

Ehiasarian and co-workers [38] noticed a significant change in the current-voltage characteristic of a magnetron when the current density at the chromium target exceeded  $600 \text{ mA/cm}^2$ . At high power densities and current density, the  $V$ - $I$ -characteristic changes dramatically, with the index in (40) to become  $q \rightarrow 1$ . Figure 1 illustrates such behavior for a tungsten target. To interpret the effect one should consider the current transport and charge generation in the discharge plasma. At the target surface the current is composed of primary ions hitting the surface and secondary electrons released, i.e.

$$I = (1 + \gamma_{SE}) I_i \quad (41)$$

where  $\gamma_{SE} = \gamma_{SE}(V_s)$  is the secondary electron yield which is a function of the primary ion energy, which in turn is determined by the sheath voltage  $V_s$ . For a fixed area one may also consider the current density and use Eq.(20), which contains the ion density  $n_i$ . An upper limit of the ion density can be estimated by the kinetic gas equation

$$n_i < n_0 = p_0/kT_0. \quad (42)$$

Using  $p_0 \approx 0.1 \text{ Pa}$  ( $\sim 1 \text{ mTorr}$ ) and  $T_0 \approx 300 \text{ K}$  (room temperature), we obtain  $n_i < 2.4 \times 10^{19} \text{ m}^{-3}$ . Putting this in Eq.(20), and using the Bohm velocity (21), one gets  $j_i < 8-10 \times 10^3 \text{ A/m}^2$ , or  $800-1000 \text{ mA/cm}^2$ . The gas temperature will be somewhat higher, and more realistic values are less than  $400 \text{ mA/cm}^2$ . The secondary electron yield for argon ions with energies less than  $1 \text{ keV}$  are generally less than unity [41]. For the purpose of an estimate one can approximate experimental data with a linear fit

$$\gamma_{SE} \approx \gamma_{pot} + \Gamma_{kin} E_i \quad (43)$$

where  $\gamma_{pot}$  is the yield of potential emission [42] at low kinetic ion energy, and  $\Gamma_{kin}$  is the factor for kinetic



emission, which is approximately constant for  $E_i < 10$  keV . The parameters  $\gamma_{pot}$  and  $\Gamma_{kin}$  are material specific. Extrapolated data by Szapiro and Rocca [41], for example, are  $\gamma_{pot} \approx 0.4$  and  $\Gamma_{kin} \approx 0.34$  keV<sup>-1</sup> for copper and  $\gamma_{pot} \approx 0.1$  and  $\Gamma_{kin} \approx 0.29$  keV<sup>-1</sup> for carbon. Using typical target voltage of about 500 V, one obtains for copper a maximum current density  $j = (1 + \gamma_{SE}) j_i \leq 700$  mA/cm<sup>2</sup>, which is very close to the threshold current density observed by Ehiasarian and co-workers [38]. The threshold current density in the example of Figure 1 is also about 600 mA/cm<sup>2</sup>. If the current exceeds this threshold for a given gas pressure, target material, and target area, the sheath voltage needs to increase in order to shift the yield of secondary electrons to higher values, Eq.(43), which allows the current (41) to increase. The situation is similar to when a “normal glow” discharge transitions into the “abnormal glow.” Secondary electrons will be accelerated in the sheath, penetrate the plasma, and can cause ionizing collisions. At the high electron energies of several 100 eV, generation of multiply charged ions is possible.

Although the changes at high current and power density appear to be strongly related to an increase in the sheath voltage, the bulk plasma has also changed fundamentally. At low current density and low degree of ionization, and neglecting the tensor character of the electric conductivity when a magnetic field is present, the electric conductivity can be expressed by [43]

$$\sigma = \frac{e^2 n_e}{m_e \sum_h \nu_{eh}} \quad (44)$$

where the summation is over all types of heavy particles electrons could collide with, and the collision frequency is given by Eq.(13). At low power density, which is typical for DC magnetron discharges, the degree of ionization is small, and the sum in Eq.(44) is dominated by electron collision with neutral atoms, not ions. In fact, the criterion

$$\sum_n \nu_{en} > \sum_i \nu_{ei} \quad (45)$$

i.e. that collisions with all kinds of neutral atoms are more frequent than collisions with all kinds of ions, can be used to define a partially ionized plasma, and the opposite relation defines a fully ionized plasma [44]. One should note that due to the long interaction length of the Coulomb potential, the degree of ionization  $\alpha$  needs only to be a few percent for a plasma to be considered fully ionized in the above sense [45]. While the conductivity of partially ionized bulk plasma depends on the electron density, see Eq.(44),

the conductivity of a fully ionized plasma is almost independent of the charge density, because the collision frequency (15) contains the charge density so that it cancels when plugged into Eq.(44). This is because in a fully ionized plasma, more free electrons could transport the current, but the number of collisions with ions is proportionally increased [4]. Therefore, even as more energy is pumped into the plasma, once fully ionized, the bulk plasma does not reduce its impedance but behaves more like an ohmic resistor for slowly varying conditions. One may suspect that the sheath voltage increase and the ohmic-like behavior of the fully ionized plasma gives rise to a coefficient  $q \rightarrow 1$  at high current and power densities.

To learn about the relative importance of these two contributions, one needs to consider the impedance of plasma and sheath. Assuming that the sheath has capacitive and ohmic contributions in parallel, and the plasma has ohmic and inductive contributions in series, with sheath and plasma being in series, one may write for the total impedance

$$\mathbf{Z} = \mathbf{Z}_{pl} + \mathbf{Z}_s = R_{pl} + i\omega L_{pl} + \frac{R_s}{1 + i\omega R_s C_s} \quad (46)$$

where  $i = \sqrt{-1}$  is the imaginary unit. For slowly changing conditions, i.e. long rise and fall times of the pulse, the ohmic contribution of a sheath can simply be interpreted as  $R_s = V_s/I$ , i.e. the ratio of sheath voltage and current. In the other extreme, at very high frequencies, in the RF and microwave region, the sheath impedance simplifies to  $1/\omega C_s$  [46]. For the relatively slow pulses in pulsed sputtering we have  $R_s < (1/\omega C_s)$  and capacitive loads may only play a role when the pulse is quickly rising.

With these considerations one can for example derive the range of useful pulse duration. The limit at long pulses is determined by the enhanced probability of arcing onset, which is typically several 10  $\mu$ s or a few 100  $\mu$ s. Pulse length also affects the average power load to the target, which must not exceed the magnetron's design specification. The limit at short pulses is given by the need to accelerate ions by the applied voltage so they can actually contribute to film growth processes in the anticipated way. That implies  $t_{pulse} \gg t_{Child}$ . In practical terms, the pulse duration must exceed a few microseconds for most plasma conditions.

In order to maximize ionization of the sputtered material, one would need to maximize the residence time of sputtered atoms in the zone of dense plasma close to the sputter target. Since dense

plasma exists only during the pulse, one would need to compare the time the sputtered atom travels through dense plasma with the pulse duration. Sputtered atoms have an initial kinetic energy  $E_{a0}$  of few eV gained in the sputter event, corresponding to a velocity of

$$u_{a0} = \sqrt{2E_{a0}/m_a} \quad (47)$$

where  $m_a$  is their mass. For example, a carbon atom of 1 eV has an initial velocity of  $u_a \approx 4000$  m/s. If there were no collisions, the path length it can cover during one pulse is simply

$$s_{a0} = u_{a0} t_p. \quad (48)$$

In our example, a sputtered carbon atom would travel 4-40 cm during the pulse duration of 10-100  $\mu$ s, i.e. it would leave the zone of dense plasma even before one pulse is completed. The key to enhanced ionization of sputtered atoms is therefore in using sufficiently high gas pressure allowing sputtered atoms to thermalize with gas atoms and ions. The mean free path, introduced with Eq.(10), must be much smaller than the characteristic size of the dense plasma near the target:  $\lambda_a \ll \ell_p$ . If we assume that the ions and electrons contribute only marginally to the total pressure, one may write the last condition as

$$p_g \gg \frac{kT_g}{\ell_p \sigma_{ag}}, \quad (49)$$

where  $T_g$  is the gas temperature, and  $\sigma_{ag}$  is the collision cross section of the sputtered atom with gas atoms. For an order of magnitude estimate one may use  $T_g \approx 400$  K,  $\sigma_{a0} \sim 10^{-18}$  m<sup>2</sup>, and  $\ell_p \approx 10^{-2}$  m, hence  $p_g \gg 1$  Pa, which is usually the case in sputtering systems.

After a sputtered atom is thermalized it may be ionized in the dense plasma during a singly pulse mainly via two mechanisms: one is via an ionizing collision with an energetic electron



and the other is via a collision with an excited gas atom (Penning ionization),



where X and G stand for the type of sputtered atom and gas atom, respectively. The superscript (\*) symbolizes the excited state. Penning ionization requires that the energy level of the excited gas atoms is higher than the ionization energy of the sputtered atoms, which is often the case with inert gases (like Ar) and sputtered metal. Hopwood and Qian [47] investigated the case of argon sputtering of aluminum with

RF-postionization; they showed that Penning ionization is dominant at low electron density while electron impact ionization becomes dominant for high electron density, with the cross-over at about  $n_e \approx 10^{11} \text{ cm}^{-3}$ .

Ionized sputtered material is of great interest to film growth because the energy of arriving ions can be tuned by biasing; however, not all ionized sputtered atoms arrive at the sheath edge near the substrate. Most of the ionized sputtered atoms have thermalized with the sputtering gas, thus they are subject to diffusion as the other heavy particles, and many of the ionized sputtered atoms may find their way back to the sheath edge of the sputter target. Those ions will be accelerated in the sheath of the magnetron target and cause sputtering of more target material, a process known as self-sputtering. If the sputter yield exceeds unity, self-sustained self-sputtering is possible, implying that the gas flow could be switched off after the process has set in. The condition of self-sustained self-sputtering can be written as [48]

$$\alpha \beta \gamma > 1 \quad (52)$$

where  $\alpha$  is the probability that a sputtered cathode atom becomes ionized,  $\beta$  is the probability that the ionized atom diffuses back to the sheath edge, and  $\gamma$  is the sputtering yield. The whole cycle is schematically shown in Fig.2. From Eq. (52) it is clear that self-sustained self-sputtering is only achievable only if  $\gamma \gg 1$ . For that reason, self-sustained self-sputtering has been experimentally verified only for a few materials of sputter yield, like copper and silver [49].

Pulsed sputtering could change this: With sufficiently high voltage pulse to the sputter target, most materials show a sputter yield exceeding unity (Fig. 3), thus many materials have the potential to switch into a qualitatively different mode that is characterized by self-sputtering and a high degree of ionization of sputtered atoms. The pulse duration must be long to allow a sputtered atom to thermalize and ionize; the ion must diffuse back to the target sheath edge, cross the sheath and impact the target surface, thereby creating at least one new sputtered atom that could repeat this cycle. The self-sputter yield of carbon is too small to fulfill condition (52) at any voltage or power. Calculations [48] have shown that the duration of a self-sputter cycle can be as short as 1  $\mu\text{s}$ , hence self-sputtering could be a common effect achieved in pulsed sputtering. One may speculate that the qualitative change in the slope of  $V$ - $I$ -characteristics, as for example shown in Fig. 1, is not only a sign for the transition to fully ionized plasma but also a “fingerprint”

of self-sputtering.

### 6.3. Pulsed filtered cathodic arc deposition

In cathodic arcs, metal plasma is produced at micron-size, non-stationary cathode spots [50]. The plasma is fully ionized and often contains ions that are multiply charged [51]. The kinetic energy of the ion's directed velocity is typically 20-150 eV, depending on the material [52], and thus ions exceed their thermal energy by more than an order of magnitude. These quite remarkable parameters are valid for dc operation; pulsing the cathodic arc discharge leads to even higher values in ion charge state [53, 54] and velocity [52]. Therefore, in applications such as film growth with substrate bias (ion plating), where ion charge state and velocity are of importance, pulsing the plasma can be advantageous. The characteristic time constant for reaching dc values in ion charge state and velocity is 50-100  $\mu\text{s}$ .

Pulsing the plasma can also have undesired effects. In between pulses, the cathode may form a thin oxide layer and components such as the chamber walls are subject to periodic particle bombardment, which can lead to plasma contamination with oxygen and water, which are incorporated in the growing film. Schneider and co-workers [55] have shown that pulsed cathodic arc plasmas can contain large fractions of hydrogen and oxygen in the first microseconds of each pulse, an effect that is particularly strong when the pulse repetition rate is low [56].

### 6.4. Metal plasma immersion ion implantation and deposition (MePIIID)

Metal plasma immersion ion implantation and deposition (MePIIID) can be understood as ion plating with pulsed bias, as was mentioned in section 5.2 above. An interesting twist is to utilize both pulsed plasma and pulsed bias, which in fact was one of the original experiments by Brown and co-workers [19] who used pulsed cathodic arcs plasmas. The advantage of pulsed arcs is to utilize the enhanced charge state number  $Q$ , which appear as a multiplier for the ion energy according to

$$E_i(Q, V_{bias}) = E_0 + QeV_{bias} , \quad (53)$$

where  $E_0$  is the kinetic energy before ion acceleration in the bias sheath. By synchronizing pulsed plasma production and pulsed high-voltage bias, metal ion implantation *without* film formation has been demonstrated [57]. If the plasma pulses are sufficiently short, bias can be applied continuously to obtain

ion implantation [58, 59].

## **7. Concluding remarks**

Pulsed plasma processing allows us to grow films much further from thermodynamic equilibrium than with continuous processing. Apart from reaching extreme pulsed plasma parameters, this is perhaps the most important feature of pulsed processing.

For example, this is particularly important for some materials such as tetrahedral amorphous carbon (ta-C). Pulsed plasma production can be used to produce plasma of high degree of ionization, which is important to produce enough energetic carbon ions via substrate bias, facilitating the subplantation growth mechanism [60, 61]. To obtain this material with very high  $sp^3$  content, the film must not be grown at elevated temperature. Here, another advantage of pulsed processing is evident, namely that the heat load can be kept small by using a suitably low duty cycle.

Pulsed plasma processing has the potential to revolutionize many of the established processes, however, the practical introduction of pulsed processes beyond R&D depends on a convincing cost-benefit analysis as well as on a good understand of this process and materials. The intention of the brief review was to point out that many effects can be interpreted by making use of well-established plasma physics.

## **Acknowledgments**

Gera Yushkov is gratefully acknowledged for his measurements of the pulsed V-I characteristic. This work was supported by the Assistant Secretary for Energy Efficiency and Renewable Energy, Office of Building Technology, of the U.S. Department of Energy under Contract No. DE-AC03-76SF00098.

## References

- [1] R. F. Bunshah, "Handbook of Deposition Technologies for Films and Coatings: Science, Technology, and Applications," 2nd ed. Park Ridge, N.J.: Noyes, 1994.
- [2] J. L. Vossen and W. Kern, *Thin Film Processes II*. Boston: Academic Press, 1991.
- [3] M. A. Lieberman and A. J. Lichtenberg, *Principles of Plasma Discharges and Materials Processing*. New York: John Wiley & Sons, 1994.
- [4] F. F. Chen, *Plasma Physics and Controlled Fusion*. New York: Plenum Press, 1984.
- [5] J. R. Roth, *Industrial Plasma Engineering. Vol. 1: Principles*. Bristol and Philadelphia: Institute of Physics Publishing, 1995.
- [6] E. W. McDaniel, *Collision Phenomena in Ionized Gases*. New York: Wiley, 1964.
- [7] J. E. Johnson, *Introduction to Atomic and Molecular Collisions*. New York: Plenum Press, 1982.
- [8] L. Spitzer, *Physics of Fully Ionized Gases*, 2nd ed. New York: Wiley, 1965.
- [9] D. Bohm, "Minimum ionic kinetic energy for a stable sheath," in *The Characteristics of Electrical Discharges in Magnetic Fields*, A. Guthrie and R. K. Wakerling, Eds. New York: McGraw-Hill, 1949, 77-86.
- [10] K.-U. Riemann, *J. Phys. D: Appl. Phys.* **24** (1991) 493.
- [11] C. D. Child, *Phys. Rev.* **32** (1911) 492.
- [12] I. Langmuir, *Phys. Rev. (Ser. II)* **2** (1913) 450.
- [13] A. T. Forrester, *Large Ion Beams*. New York: Wiley, 1988.
- [14] W. D. Munz, D. Schulze, and F. J. M. Hauzer, *Surf. Coat. Technol.* **50** (1992) 169.
- [15] D. M. Mattox, *J. Vac. Sci. Technol.* **10** (1973) 47.
- [16] R. J. Adler and S. T. Picraux, *Nucl. Instrum. Meth. Phys. Res. B* **6** (1985) 123.
- [17] J. R. Conrad, J. L. Radtke, R. A. Dodd, F. J. Worzala, and N. C. Tran, *J. Appl. Phys.* **62** (1987) 4591.
- [18] B. Mizuno, I. Nakayama, N. Aoi, M. Kubota, and T. Komeda, *Appl. Phys. Lett.* **53** (1988) 2059.
- [19] I. G. Brown, X. Godechot, and K. M. Yu, *Appl. Phys. Lett.* **58** (1991) 1392.
- [20] W. Olbrich, J. Fessmann, G. Kampschulte, and J. Ebberink, *Surf. Coat. Technol.* **49** (1991) 258.
- [21] W. Olbrich and G. Kampschulte, *Surf. Coat. Technol.* **61** (1993) 2627.
- [22] O. R. Monteiro, *Annual Rev. Mat. Sci.* **31** (2001) 111.

- [23] A. Anders, "Handbook of Plasma Immersion Ion Implantation and Deposition," New York: Wiley, 2000.
- [24] A. Anders, *Surf. Coat. Technol.* **93** (1997) 157.
- [25] A. Anders, *Vacuum* **67** (2002) 673.
- [26] J. R. Conrad, *J. Appl. Phys.* **62** (1987) 777.
- [27] M. A. Lieberman, *J. Appl. Phys.* **66** (1989) 2926.
- [28] B. P. Wood, D. J. Rej, A. Anders, I. G. Brown, R. J. Faehl, S. M. Malik, and C. P. Munson, "Fundamentals of plasma immersion ion implantation," in *Handbook of Plasma Immersion Ion Implantation and Deposition*, A. Anders, Ed. New York: Wiley, 2000, chapter 4.
- [29] B. P. Wood, *J. Appl. Phys.* **73** (1993) 4770.
- [30] M. Nastasi, X.-M. He, K. C. Walter, M. Hakovirta, and M. Trkula, *Surf. Coat. Technol.* **136** (2001) 162.
- [31] K. C. Walter and M. Nastasi, *Surf. Coat. Technol.* **156** (2002) 306.
- [32] K. M. He, M. Hakovirta, A. M. Peters, B. Taylor, and M. Nastasi, *J. Vac. Sci. Technol. A* **20** (2002) 638.
- [33] A. M. Peters and M. Nastasi, *Vacuum* **67** (2002) 169.
- [34] J. Wöhle, C. Pfohl, K.-T. Rie, A. Gebauer-Teichmann, and S. K. Kim, *Surf. Coat. Technol.* **131** (2000) 127.
- [35] V. Kouznetsov, K. Macak, J. M. Schneider, U. Helmersson, and I. Petrov, *Surf. Coat. Technol.* **122** (1999) 290.
- [36] S. M. Rossnagel, *J. Vac. Sci. Technol. B* **16** (1998) 2585.
- [37] K. Macak, V. Kouznetsov, J. Schneider, U. Helmersson, and I. Petrov, *J. Vac. Sci. Technol. A* **18** (2000) 1533.
- [38] A. P. Ehasarian, R. New, W.-D. Münz, L. Hultman, U. Helmersson, and V. Kouznetsov, *Vacuum* **65** (2002) 147-154.
- [39] I. Petrov, A. Myers, J. E. Greene, and J. R. Abelson, *J. Vac. Sci. Technol. A* **12** (1994) 2846.
- [40] A. Anders, *Appl. Phys. Lett.* **76** (2000) 28.
- [41] B. Szapiro and J. J. Rocca, *J. Appl. Phys.* **65** (1989) 3713.
- [42] M. Kamimsky, *Atomic and Ionic Impact Phenomena on Metal Surfaces*. Berlin: Springer-Verlag, 1965.
- [43] M. Mitchner and C. H. Kruger, *Partially Ionized Gases*. New York: Wiley, 1973.



- [44] V. E. Golant, A. P. Zhilinsky, and I. E. Sakharov, *Fundamentals of Plasma Physics*. New York: Wiley, 1980.
- [45] F. Cap, *Introduction to Plasma Physics I. Theoretical Foundation*, 2nd ed. Berlin: Akademie-Verlag, 1975.
- [46] W. Schwarzenbach, A. A. Howling, M. Fivaz, S. Brunner, and C. Hollenstein, *J. Vac. Sci. Technol. A* **14** (1996) 132.
- [47] J. Hopwood and F. Qian, *J. Appl. Phys.* **78** (1995) 758.
- [48] A. Anders, S. Anders, M. A. Gundersen, and A. M. Martsinovskii, *IEEE Trans. Plasma Sci.* **23** (1995) 275.
- [49] W. M. Posadowski, *Vacuum* **46** (1995) 1017.
- [50] B. Jüttner, *J. Phys. D: Appl. Phys.* **34** (2001) R103.
- [51] I. G. Brown, *Rev. Sci. Instrum.* **65** (1994) 3061.
- [52] A. Anders and G. Y. Yushkov, *J. Appl. Phys.* **91** (2002) 4824.
- [53] A. Anders, *IEEE Trans. Plasma Sci.* **26** (1998) 118.
- [54] A. Anders, S. Anders, B. Jüttner, and I. G. Brown, *IEEE Trans. Plasma Sci.* **PS-21** (1993) 305.
- [55] J. M. Schneider, A. Anders, I. G. Brown, B. Hjörvarsson, and L. Hultman, *Appl. Phys. Lett.* **75** (1999) 612.
- [56] G. Y. Yushkov and A. Anders, *IEEE Trans. Plasma Sci.* **26** (1998) 220.
- [57] B. P. Wood, W. A. Reass, and I. Henins, *Surf. Coat. Technol.* **85** (1996) 70.
- [58] T. Sroda, S. Meassick, and C. Chan, *Appl. Phys. Lett.* **60** (1992) 1076.
- [59] Z. Xia, C. Chan, S. Meassick, and R. Purser, *J. Vac. Sci. Technol. B* **13** (1995) 1999.
- [60] Y. Lifshitz, S. R. Kasai, J. W. Rabalais, and W. Eckstein, *Phys. Rev. B* **41** (1990) 10468.
- [61] S. Uhlmann, T. Fraunheim, and Y. Lifshitz, *Phys. Rev. Lett.* **81** (1998) 641.

Table 1. Examples of dimensionless parameters relevant to pulsed plasma processing; symbols have their usual meaning as defined in the text.

Name of parameter	Definition	Remarks
degree of ionization	$\alpha = \frac{n_i}{n_i + n_0}$	High $\alpha$ implies effectiveness of bias
Knudsen number	$Kn = \lambda/\ell$	Ratio of mean free path $\lambda$ to characteristic length $\ell$
Hall parameter	$H = \frac{eB}{m\nu}$	Ratio of gyration frequency to collision frequency
pulse duty cycle	$\delta = \frac{t_{on}}{t_{on} + t_{off}}$	$\delta \rightarrow 1$ corresponds to DC bias
pulse rise parameter	$\tau_{rise} = t_{rise} \omega_{pl,i}$	for $\tau_{rise} \rightarrow 0$ ion matrix sheath forms
pulse form factor	$\varphi = \frac{t_{flat}}{t_{pulse}}$	$\varphi \rightarrow 1$ for a rectangular pulse

### **Figure Captions**

Fig. 1 Example of a current-voltage characteristics for DC and pulsed magnetron sputtering. Parameters: 1.5" W target, Ar at about 1 Pa.

Fig. 2 Schematic of the cycle of self-sustained self-sputtering.

Fig. 3 Self-sputter yield of target materials as a function of self-ion kinetic energy, which is determined by the voltage to the sputter target (Monte Carlo simulation using code T-DYN v.4.0).

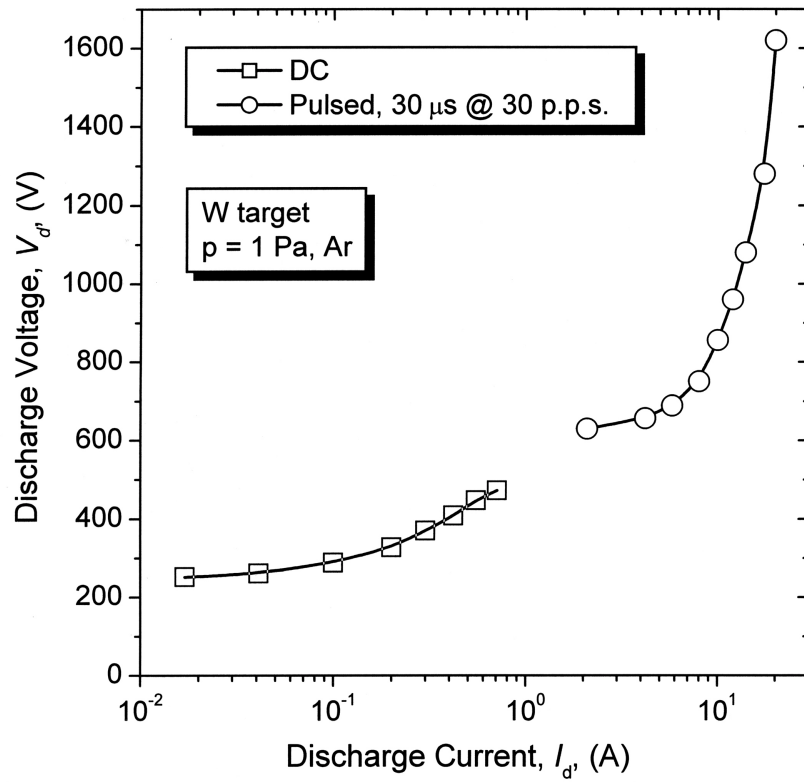


Fig. 1

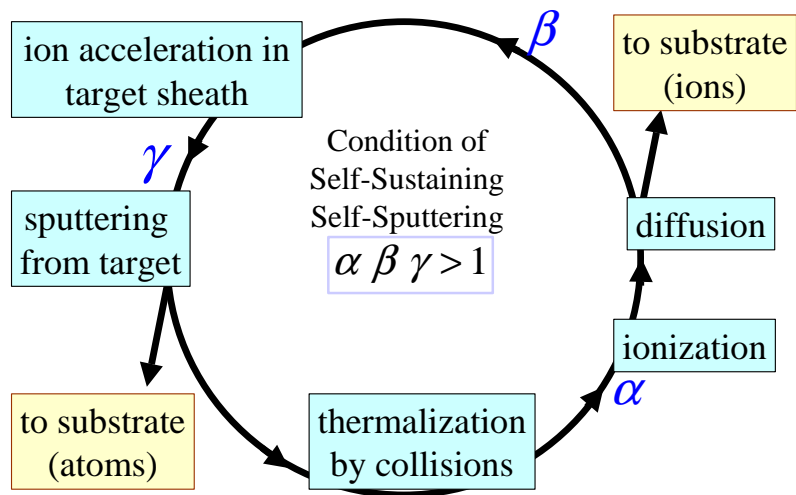


Fig. 2

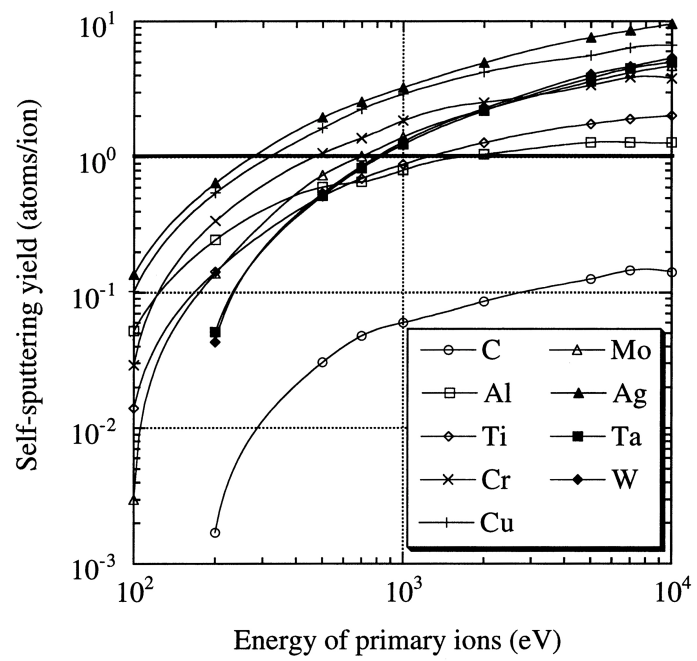


Fig. 3